

## Original Article

## Antidiabetes study of *Spondias mombin* (Linn) stem bark fractions in high-sucrose diet-induced diabetes in *Drosophila melanogaster*

Damilola A. Omoboyowa, PhD<sup>a,\*</sup>, Mary D. Agoi, M.sc<sup>a</sup>, Sidiqat A. Shodehinde, PhD<sup>a</sup>, Oluwatosin A. Saibu, M.sc<sup>b</sup> and Jamiyu A. Saliu, PhD<sup>a</sup>

<sup>a</sup> Department of Biochemistry, Adekunle Ajasin University, Akungba-Akoko, Ondo State, Nigeria

<sup>b</sup> Department of Environmental Toxicology, Universitat Duisburg-Essen, NorthRhine-Westphalia, Germany

Received 30 September 2022; revised 29 November 2022; accepted 18 January 2023; Available online 29 January 2023



### المخلص

**أهداف البحث:** ارتبط ظهور مرض السكري المقاوم للإنسولين بنظام غذائي عالي السكر في الفئاريات واللافقاريات. من ناحية أخرى، تم الإبلاغ عن أن جزءاً مختلفاً من نبات "سبوندياس مومبين" يمتلك إمكانات مضادة لمرض السكري. ومع ذلك، لم يتم استكشاف الفعالية المضادة لمرض السكري لحاء جذع "سبوندياس مومبين" في نظام غذائي عالي السكر الناتج عن نموذج ذبابة الفاكهة السوداء البطن. في هذه الدراسة الحالية، تم إجراء التأثيرات المضادة للسكري ومضادات الأكسدة لكسور المذيبات من اللحاء.

**طريقة البحث:** تم إجراء تجزئة متتالية لمستخلص الإيثانول لحاء الساق "سبوندياس مومبين" وتم إخضاع الكسور الناتجة لمقاييسات مضادات الأكسدة ومضادات السكري في المختبر باستخدام البروتوكولات القياسية. تم تثبيت المركبات النشطة التي تم تحديدها باستخدام جهاز الاستشراب السائل الرفيع الإنجاز لدراسة جزء "بيوتانول" على الموقع النشط لـ "ألفا-أميلاز" في ذبابة الفاكهة باستخدام برنامج "أوتودوك" لمحاكاة النمذجة الجزيئية. تم دمج أجزاء "بيوتانول" و "إيثيل الأسيتات" من النبات في النظام الغذائي لمرض السكري والذباب غير المصاب بالسكري لدراسة الخصائص المضادة لمرض السكري ومضادات الأكسدة في الجسم الحي.

**النتائج:** أظهرت النتائج التي تم الحصول عليها أن جزيئات "ن-بيوتانول" و "إيثيل الأسيتات" تمتلك أعلى قدرة مضادة للأكسدة في المختبر عن طريق تثبيط "دي.بي.بي.تش" و "اف.أ.بي" وجذر الهيدروكسيل متبوعاً بتثبيط معنوي لـ "ألفا-أميلاز". يكشف تحليل الاستشراب السائل الرفيع الإنجاز عن تحديد ثمانية مركبات تحتوي على كيرسيتين ذات أعلى قيمة تليها روتين، ورامنيستين، وحمض الكوروجينيك، وزينوكسانثين، ولوتين، وإيزوكيرسيتين، وروتينوز تظهر أدنى

قيمة. أعادت الكسور اختلال توازن الجلوكوز ومضادات الأكسدة في داء السكري وهو ما يمكن مقارنته بالعقار القياسي (الميتفورمين). كانت الكسور أيضاً قادرة على تنظيم تعبير "أي.ال.بي-2" و "أي.ان.ار" و "أي.ام.بي.ال2" في ذباب السكري. كشفت دراسات السيليكو عن القدرة التثبيطية للمركبات النشطة ضد الأميلاز مع أيزوكيرسيتين، ورامنيستين، وروتين، وكيرسيتين، وحمض الكوروجينيك التي لها تقارب ارتباط أعلى من الدواء القياسي (أكاربوز).

**الاستنتاجات:** بشكل عام، تعمل كسور البيوتانول والإيثيل أسيتات من لحاء "سبوندياس مومبين" على تحسين مرض السكري من النوع 2 في ذبابة الفاكهة. ومع ذلك، تم اقتراح مزيد من الدراسة المضادة للسكري في نموذج حيواني آخر لتكتمل هذه النتيجة.

**الكلمات المفتاحية:** ذبابة الفاكهة؛ سبوندياس مومبين؛ السكري؛ مضادات الأكسدة؛ في المختبر؛ في السيليكو؛ في الجسم الحي

### Abstract

**Objective:** The onset of insulin resistant diabetes has been associated with a high-sucrose diet in vertebrates and invertebrates. However, various parts of *Spondias mombin* reportedly possess antidiabetic potential. However, the antidiabetic efficacy of *S. mombin* stem bark in high-sucrose diet-induced *Drosophila melanogaster* model has not been explored. In this study, the antidiabetic and antioxidant effects of the solvent fractions of *S. mombin* stem bark were evaluated using *in vitro*, *in vivo*, and *in silico* methods.

**Methods:** Successive fractionation of *S. mombin* stem bark ethanol extract was performed; the resulting fractions were subjected to *in vitro* antioxidant and antidiabetic assays using standard protocols. The active compounds identified from the high-performance liquid chromatography (HPLC) study of the n-butanol fraction were docked against the active site of *Drosophila α-*

\* Corresponding address. Department of Biochemistry, Adekunle Ajasin University, Akungba-Akoko, Ondo State, Nigeria

E-mail: damilola.omoboyowa@aaau.edu.ng (D.A. Omoboyowa)

Peer review under responsibility of Taibah University.



amylase using AutoDoc Vina. The n-butanol and ethyl acetate fractions of the plant were incorporated into the diet of diabetic and nondiabetic flies to study the *in vivo* antidiabetic and antioxidant properties.

**Results:** The results obtained revealed that n-butanol and ethyl acetate fractions had the highest *in vitro* antioxidant capacity by inhibiting 2,2-diphenyl-1-picrylhydrazyl (DPPH), ferric reducing antioxidant power, and hydroxyl radical followed by significant inhibition of  $\alpha$ -amylase. HPLC analysis revealed the identification of eight compounds with quercetin having the highest peak followed by rutin, rhamnetin, chlorogenic acid, zeinoxanthin, lutein, isoquercetin, and rutinose showing the lowest peak. The fractions restored the glucose and antioxidant imbalance in diabetic flies, which is comparable with the standard drug (metformin). The fractions were also able to upregulate the mRNA expression of insulin-like peptide 2, insulin receptor, and ecdysone-inducible gene 2 in diabetic flies. The *in silico* studies revealed the inhibitory potential of active compounds against  $\alpha$ -amylase with isoquercetin, rhamnetin, rutin, quercetin, and chlorogenic acid having higher binding affinity than the standard drug (acarbose).

**Conclusion:** Overall, the butanol and ethyl acetate fractions of *S. mombin* stem bark ameliorate type 2 diabetes in *Drosophila*. However, further studies are needed in other animal models to confirm the antidiabetes effect of the plant.

**Keywords:** Antioxidant; Diabetes; *Drosophila*; *In silico*; *In vitro*; *In vivo*

© 2023 The Authors.

Production and hosting by Elsevier Ltd on behalf of Taibah University. This is an open access article under the CC BY-NC-ND license (<http://creativecommons.org/licenses/by-nc-nd/4.0/>).

## Introduction

Diabetes is a metabolic disease characterized by high blood glucose (hyperglycemia) resulting from insulin deficiency, insulin resistance, or both.<sup>1</sup> Diabetes mellitus (DM) is associated with the abnormal metabolism of fats, carbohydrates, and proteins,<sup>2</sup> and often leads to complications such as peripheral neuropathy, retinopathy, coronary heart disease, and cataracts.<sup>3,4</sup> Chronic hyperglycemia causes glucose autooxidation and protein glycosylation, resulting in the generation of reactive oxygen species (ROS).<sup>4</sup>

Dietary sugar remains the major source of glucose in the body; this sugar is converted to monosaccharides in the body before absorption and transportation by the blood to cells and tissues for metabolism.<sup>5</sup> However, excess sugar disrupts glucose homeostasis in the body causing obesity, which can lead to other metabolic disorders such as fatty liver, hypertension, and eventually the onset of type 2 DM.<sup>6</sup> The diabetes-induced *Drosophila melanogaster* (fruit fly) model is an excellent experimental model for studying type 2

diabetes, because 74% of human disease-related genes are conserved in the fly.<sup>5</sup> In particular, glucose-metabolizing genes are highly conserved between mammals and fruit flies.<sup>7</sup> The unwanted side effects and cost of available oral hypoglycemic drugs and insulin injection for diabetes management have shifted the research focus to natural products as sources of antidiabetic therapy.

*Spondias mombin* (Linn) belongs to the family of Anacardiaceae, commonly known as the Hog plum; the plant is locally called Iyeye, Olosan (Yoruba), and Uvuru (Igbo) in Nigeria; Ubo in Peru; and Hobo in Mexico.<sup>8</sup> In herbal medicine, *S. mombin* is used traditionally for the treatment of gastrointestinal disorders such as diarrhea.<sup>9</sup> The antidiabetic potential of *S. mombin* leaves has been reported in alloxan-induced rats<sup>10</sup> and streptozotocin-induced diabetic rats.<sup>11</sup> The hypoglycemic effect of *S. mombin* stem bark has been reported in healthy rats.<sup>12</sup> After establishing high-sucrose diet (HSD)-induced diabetes in *Drosophila* as in previous studies,<sup>5,13</sup> this study investigated the antidiabetic potential of ethyl acetate and n-butanol fractions of *S. mombin* stem bark in this HSD-induced *Drosophila* model.

## Materials and Methods

### Plant materials

The stem bark of *S. mombin* (Linn) was removed from a tree with a clean knife at the medicinal garden of Adekunle Ajasin University, Akungba-Akoko (Ondo State, Nigeria). Authentication of the plant was done by Dr. Obembe from the Plant Science and Biotechnology Departmental Herbarium (PSBH) of our institution. The voucher specimen with voucher number V/No. PSBH-222 was deposited at the Herbarium.

### Culture of fly stock

*D. melanogaster* (Harwich strain) used for this study was collected from the *Drosophila* Laboratory of Biochemistry Department, University of Ibadan (Oyo State, Nigeria). The flies were maintained at  $25 \pm 2$  °C at the Phytomedicine and Functional Food Laboratory of the Biochemistry Department of our institution. The fly diet was composed of cornmeal, agar–agar, Brewer's yeast, and Nipagin (preservative).

## Methods

### Extraction and solvent-partitioned fractionation of crude ethanol extract

The stem bark of *S. mombin* was dried in a cool environment for 28 days and powdered using a mechanical blender. The ethanol extract was obtained by soaking 115 g powdered sample with 1000 mL ethanol for 72 h. The extract was filtered to remove the insolubilized portion. The solvent was removed from the filtrate by concentration using a rotary evaporator. The *S. mombin* extract (45 g) was dissolved in distilled water (500 mL), and extracted with four solvents according to increasing order of polarity. Hexane was used

to partition the extract from water for the n-hexane fraction of *S. mombin* (HSM), followed by ethyl acetate for the ethyl acetate fraction of *S. mombin* (ESM). The aqueous portion was also partitioned with n-butanol for the n-butanol fraction of *S. mombin* (BSM) and the resultant aqueous fraction of *S. mombin* (ASM).

#### In vitro antioxidant assay

##### Determination of ferric reducing antioxidant potential

The ferric reducing antioxidant potential (FRAP) was assayed according to the procedure of reduction of  $\text{Fe}^{3+}$ -triipyridyltriazine to  $\text{Fe}^{2+}$ -triipyridyltriazine at alkaline pH using the antioxidant ability of the tested sample.<sup>14</sup> The FRAP assay for fractions was carried out according to the Benzie and Strain method.<sup>14</sup> Briefly, freshly prepared FRAP working reagent was prepared consisting of acetate buffer (25 mL), 2,4,6-triipyridyl-s-troazine (2.5 mL) solution, and ferric chloride (10:1:1), and the mixture was used at 37 °C. The reaction mixture was made of 0.2 mL fractions and 2.8 mL working reagent, and kept in the dark for 30 min at 27 °C. The absorbance was read at 593 nm, and the FRAP concentration was estimated from the standard curve of ferrous sulphate and calculated in  $\text{mMFe}^{2+}$ .

##### 1,1-Diphenyl-2-picrylhydrazyl scavenging activity

The scavenging capacity of 1,1-diphenyl-2-picrylhydrazyl (DPPH) of the fractions was evaluated according to the procedure described by Omoboyowa et al.<sup>15</sup> with slight modification. Briefly, 1 mL of 250–1000  $\mu\text{g/mL}$  of the tested compounds was added to 1 mL DPPH reagent (2.4 mg DPPH prepared with 200 mL methanol). The mixture was mixed thoroughly and allowed to stand in the dark for 30 min. The absorbance was read at 517 nm, and the percentage DPPH inhibition was evaluated as:

##### Percentage DPPH inhibition

$$= \frac{\text{Absorbance of control} - \text{Absorbance of sample}}{\text{Absorbance of control}} \times 100$$

#### In vitro hydroxyl radical inhibitory activity

The inhibitory ability of hydroxyl (OH) radicals was estimated as described by Kunchandy and Rao.<sup>16</sup> Briefly, 1.0 mL working reagent comprising 100  $\mu\text{L}$  of 28 mM of deoxyribose prepared with 20 mM potassium phosphate buffer (pH 7.4), 500  $\mu\text{L}$  of fractions, 200  $\mu\text{M}$   $\text{FeCl}_3$  (1:1 v/v), 200  $\mu\text{L}$  of EDTA (1.04 mM), 100  $\mu\text{L}$  of  $\text{H}_2\text{O}_2$  (1.0 mM), and 100  $\mu\text{L}$  of ascorbic acid (1.0 mM) was allowed to stand for 1 h at 37 °C. Then 1.0 mL of 1% thiobarbituric acid and 1.0 mL of 2.8% trichloroacetic acid were added and allowed to stand for 20 min at 100 °C. The mixture was allowed to cool, and the absorbance was read at 532 nm against the blank sample.

#### In vitro assay of $\alpha$ -amylase inhibition

Inhibition of  $\alpha$ -amylase of the fractions was evaluated according to the method of Worthington.<sup>17</sup> The fractions were diluted as appropriate and added to 500  $\mu\text{L}$  of 0.2–

1.0 mg/mL, 500  $\mu\text{L}$  of 0.02 M sodium phosphate buffer (pH 6.9) prepared with 0.006 M NaCl, and 0.5 mg/mL  $\alpha$ -amylase solution; the mixture was allowed to stand at 27 °C for 10 min. Then 500  $\mu\text{L}$  of 1% starch solution in sodium phosphate buffer (pH 6.9) was added. The mixture was allowed to stand for 10 min at 25 °C. Next, 1.0 mL of 96 mM dinitrosalicylic acid was added to stop the reaction. The mixture was boiled for 5 min and cooled before the absorbance was read at 540 nm. The percentage inhibition was estimated using the following formula:

$$\text{Inhibition percentage} = \frac{\text{Abs of control} - \text{Abs of sample}}{\text{Abs of control}} \times 100$$

#### High-performance liquid chromatography analysis

The n-butanol fraction was found to be the most active fraction based on the *in vitro*  $\alpha$ -amylase inhibitory study. Therefore, the BSM was subjected to HPLC analysis (Shimadzu Co., Kyoto, Japan) with a fluorescence detector (RF-10AXL), Prominence autosampler (SIL-20AHT; Shimadzu), Prominence pump (LC-20AD; Shimadzu), Hypersil GOLD column (4.6  $\times$  250 cm, 5  $\mu\text{m}$ ; Thermo Fisher Scientific, Waltham, MA, USA), and column oven (CTO-10ASvp; Shimadzu). The syringe filter was used to filter the samples (fraction and reference compounds). Then 50  $\mu\text{L}$  filtrate from each sample was inserted at a flow rate of 1 mL/min and running time of 50 min. To prepare the sample, 10 g n-butanol fraction was dissolved in an amber bottle with 20 mL acetonitrile/methanol. The mixture was vigorously shaken for 30 min. After shaking, the organic solvent was decanted into a 25 mL standard flask and filled up to the mark. Standard analytes were initially inserted into a chromatograph to generate a chromatogram with a peak profile used to create a window in the HPLC machine for analysis of the test sample. Then an aliquot of the sample (BSM) was inserted into the chromatograph to generate a corresponding peak profile of the sample in the chromatogram. The peak area and retention time of the sample were compared to those of the reference sample relative to the concentration obtain for the sample using the following formula:

##### Concentration of sample

$$= \frac{\text{Peak of sample} \times \text{standard concentration}}{\text{peak area of the standard}}$$

#### Survival assay

Approximately 3- to 4-day old flies were transferred under mild anesthesia using ice from culture vials, and separated into five different groups of 30 flies. The flies were always transferred at 5-day intervals into new diet vials for a period of 45 days to ensure good quality of diet throughout the experiment. The effects of the fractions on fly survival were investigated with a pilot study to determine the concentration of the fractions used.

Group 1: Normal diet group; 1 mL EtOH/10 g diet

- Group 2: 1 mg BSM/10 g diet
- Group 3: 2 mg BSM/10 g diet
- Group 4: 3 mg BSM/10 g diet
- Group 5: 1 mg ESM/10 g diet
- Group 6: 2 mg ESM/10 g diet
- Group 7: 3 mg ESM/10 g diet

The BSM and ESM concentrations were added to the fly diet every 5 days for 45 days and fly mortality was documented daily for 45 days.

#### *Induction of diabetes in flies using sucrose*

Induction of type 2 diabetes in fruit flies was carried out by a protocol reported by Omale et al.<sup>13</sup> with slight modifications. Briefly, 2.5 g sucrose/10 g diet was added to the normal diet of the fly with other diet components remaining constant (1% agar, 3.4% yeast, 8.3% cornmeal, and 1% nipagin) to induce diabetes in the Harwich strain of *D. melanogaster*. The flies were exposed to sucrose incorporated in the diet for 10 days and observed for diabetes symptoms such as low rate of L3 larvae emergence, decreased body size, and decreased locomotive activities.

#### *Treatment of sucrose-induced flies with active fractions*

To investigate the antidiabetic activity of ESM and BSM in *D. melanogaster*, diabetes-induced flies were placed on fractions incorporating the diet, and metformin served as reference drug for 10 days according to the design below. Thirty-five flies were included in each group with four replicates.

- Group 1: Normal diet
- Group 2: Normal flies exposed to 4.0 mg BSM/10 g diet
- Group 3: Normal flies exposed to 4.0 mg ESM/10 g diet
- Group 4: Diabetes flies exposed to 1 mL ethanol/10 g diet
- Group 5: Diabetes flies exposed to 16 mg metformin/10 g diet
- Group 6: Diabetes flies exposed to 2.0 mg BSM/10 g diet
- Group 7: Diabetes flies exposed to 4.0 mg BSM/10 g diet
- Group 8: Diabetes flies exposed to 2.0 mg ESM/10 g diet
- Group 9: Diabetes flies exposed to 4.0 mg ESM/10 g diet

After 10 days of treatment, the flies were anesthetized using ethanol, allowed to blot-dry, and weighed using 0.1 M phosphate buffer (pH 7.0) to homogenize the flies at a ratio of 1 mg flies to 10  $\mu$ L buffer. The homogenates were centrifuged for 10 min at 4000 $\times$ g. Then the supernatants were separated from the pellets and used for *in vivo* antioxidant and glucose concentration assays.

#### *Locomotor assay*

The negative geotaxis assay method was used for the locomotor assay.<sup>18</sup> Ten normal flies and experimental flies were briefly anesthetized under ice and transferred to a 15  $\times$  15 cm glass column. After recovery, the flies were gently tapped down the column. The number of flies that were able to

climb up to the 6 cm mark was recorded. The percentage negative geotaxis was estimated using the following formula:

$$\% \text{ negative geotaxis} = \frac{\text{Total No of flies} - \text{No of flies that climb above 6 cm}}{\text{Total No of flies}} \times 100$$

#### *Estimation of glucose concentration*

The assay for determining the concentration of glucose in the fly homogenate was conducted according to the procedure of Trinder,<sup>19</sup> using the Agappe LiquiCHEK Kit.

#### *Estimation of total thiol content*

The total thiol content of the fly homogenate was estimated by the procedure of Adedara et al.<sup>18</sup> with modifications. The working reagent consisted of 1700  $\mu$ L potassium phosphate buffer (0.1 M; pH 7.4), 200  $\mu$ L homogenates, and 100  $\mu$ L of 5,5'-dithiobis-(2-nitrobenzoic acid). The mixture was allowed to stand for 30 min at 27  $^{\circ}$ C. The absorbance was read at 412 nm. The standard used was reduced glutathione, and the results are presented as  $\mu$ mol/mg of protein.

#### *Estimation of nitric oxide level*

The nitric oxide (NO) concentration was estimated by the Griess reaction procedure as reported by Green et al.<sup>20</sup> The mixture of homogenate and Griess solution was allowed to stand for 20 min at 27  $^{\circ}$ C. Thereafter, the absorbance was read at 550 nm. The level of NO in the mixture was extrapolated from the NaNO<sub>2</sub> calibration curve.

#### *Assay of lipid peroxidation assay*

The assay for lipid peroxidation level was performed according to the procedure described by Ohkawa et al.<sup>21</sup> The reagent mixture consisted of 5  $\mu$ L of 10 mM butylhydroxytoluene (BHT), 200  $\mu$ L thiobarbituric acid (0.67%), 600  $\mu$ L of 1% *O*-phosphoric acid, distilled water (105  $\mu$ L), and fly homogenate (90  $\mu$ L). The mixture was allowed to stand for 45 min at 90  $^{\circ}$ C, and the absorbance was read at 535 nm. The results were calculated as  $\mu$ mol of malondialdehyde/ $\mu$ L.

#### *Total RNA extraction and cDNA conversion*

RNA was extracted from the whole drosophila homogenates with the Quick-RNA MiniPrep™ Kit (Zymo Research International, Tustin, CA, USA). DNase I (Cat: M0303S; New England Biolabs [NEB], Ipswich, MA, USA) treatment was used to remove DNA contaminants from the isolated RNA. The RNA was quantified at 260 nm and the purity was confirmed at 260 and 280 nm using the A&E Spectrophotometer (A & E Lab (UK) Co. Ltd., London, UK). DNA-free RNA (1  $\mu$ g) was converted by reverse transcriptase reaction to cDNA using the ProtoScript II First Strand cDNA Synthesis Kit (NEB) based on a three-

step reaction: 65 °C for 5 min, 42 °C for 1 h, and 80 °C for 5 min.<sup>22</sup>

#### Gene amplification by PCR and agarose gel electrophoresis

Polymerase chain reaction (PCR) for amplification of insulin-like peptide 2 (ILP2), insulin receptor (InR), and ecdysone-inducible gene 2 (IMPL2) genes was performed with the OneTaqR2X Master Mix using the following primers (Inqaba Biotec, Pretoria, South Africa): set: >NM\_079288.3 *Drosophila* ILP2, forward primer: AGGTGCTGAG-TATGGTGTGC, reverse primer: TGTCGGCACCGGG-CAT, >NM\_00-1274480.1 *Drosophila* ImpL2, transcript variant D, forward primer TGCCGGCTTAGA-CACTAATTT, reverse primer GCTGCCTGAATCGC-TAGGAA, >NM\_001144622.2 *Drosophila* InR, forward primer TTTGTGCCTCGCA-CTTTGC, reverse primer ATACGCTCACCAACACATGC. >NM\_001273184.2 *Drosophila* GPDH, transcript variant G, forward primer TCGGACTGCGTAGACACTAGA, reverse primer AGCGCCATCTATGTAAGGATGT was used as the housekeeping gene. PCR amplification was performed in 25 µL reaction reagent consisting of cDNA, primer (forward and reverse), and Ready Mix Taq PCR master mix under the following condition: starting denaturation at 95 °C for 5 min, 30 cycles of amplification (denaturation at 95 °C for 30 s, annealing for 30 s, and extension at 72 °C for 60 s) and ending with final extension at 72 °C for 10 min. The amplicons were resolved on a 1.0% agarose gel. The GAPDH gene was required to normalize the relative expression level of each gene, and intensity of the band was quantified with ImageJ software.<sup>22</sup>

#### In silico study

Bioactive compounds that were identified from HPLC analysis of BSM were retrieved from the PubChem database (<https://pubchem.ncbi.nlm.nih.gov>). The protein ( $\alpha$ -amylase [2QV4]) was retrieved from <http://rcsb.org>. Eight compounds identified from *S. mombin* and reference drug were virtually screened against the binding site of the protein using the catalytic site of the ligand co-crystallized with the protein to generate a grid coordinate of  $x = 39.01$ ,  $y = 31.15$ ,  $z = 24.00$ . Virtual screening of the compounds against the protein was performed using AutoDock 4.0 via PyRx.<sup>23</sup> The protein and compounds were prepared before docking. Co-crystallized molecule of the protein was extracted, prepared, and redocked into the same binding domain of the proteins for validation of the screening procedure.<sup>24</sup> The visualization and conversion of protein-ligand complexes to two-dimensional format was performed by using Discovery Studio 2020.

#### Statistical analyses

The statistical analyses of the data obtained were carried out by GraphPad Prism 9, and the survival rate was analyzed by the Kaplan–Meier's method. Log-rank tests were used for the mean comparisons. For the biochemical data, one

way analysis of variance was used for the data analyses, followed by Dunnett's post hoc test.  $P < 0.05$  was considered statistically significant.

## Results and discussion

### In vitro antioxidant activity

Plants have always been an excellent source of drugs for many metabolic disorders such as diabetes and cancer, and many currently used drugs are derived directly or indirectly from medicinal plants.<sup>25</sup> *S. mombin* is widely known for its pharmacological benefits. The anticancer potential of carotenoid isolates from the leaves of *S. mombin* has been documented by Metibemu et al.<sup>26</sup> Although previous studies have reported the antidiabetic activity of *S. mombin* leaves,<sup>10,11</sup> the antidiabetic efficacy of solvent fractions of *S. mombin* stem bark in the HSD-induced diabetes *Drosophila* model has not been explored.

Free radicals are key players in the pathogenesis of various metabolic disorders; therefore, the anti-oxidant potency of natural products has been attributed to their therapeutic properties. Investigation of the *in vitro* free radical inhibiting capacity of *S. mombin* stem bark via DPPH, OH scavenging activity, and FRAP (Figure 1a–c) revealed that ESM and BSM possessed appreciable free radical scavenging potential. The DPPH assay estimates the potential of natural compounds to release proton to convert DPPH salt to its reduced form (diphenylpicrylhydrazine).<sup>27</sup> The high DPPH-scavenging power of n-butanol might be associated with the presence of polyphenols, as evident in the HPLC analysis (Figure 3). Ascorbic acid and galic acid were used as standards for hydroxyl radical inhibition and percentage DPPH inhibition, respectively, because Omoboyowa et al.<sup>28</sup> reported the *in vitro* antioxidant power of both compounds. The ferric-reducing antioxidant power of the fractions is represented in Figure 1c; the results showed that BSM had the highest ferric-reducing power. The results from this study are consistent with the observations of Boni et al.,<sup>29</sup> who reported the *in vitro* antioxidant potential of methanol and water extracts of *S. mombin* stem bark.

### In vitro $\alpha$ -amylase inhibition assay

One of the major ways to control blood sugar level is by delaying its absorption, which is achieved by inhibiting carbohydrate-hydrolyzing proteins including  $\alpha$ -amylase present in the small intestine. This enzymatic inhibition slows down carbohydrate digestion and monosaccharide absorption, thereby reducing the postprandial glucose level.<sup>30</sup> The present study showed the inhibitory effect of *S. mombin* stem bark (HSM, ESM, BSM and ASM) in Figure 2. The results showed that, across the concentrations of the fractions used, BSM and ESM significantly ( $P < 0.05$ ) inhibited  $\alpha$ -amylase activity compared to ASM and HSM. Hence, the reason for their

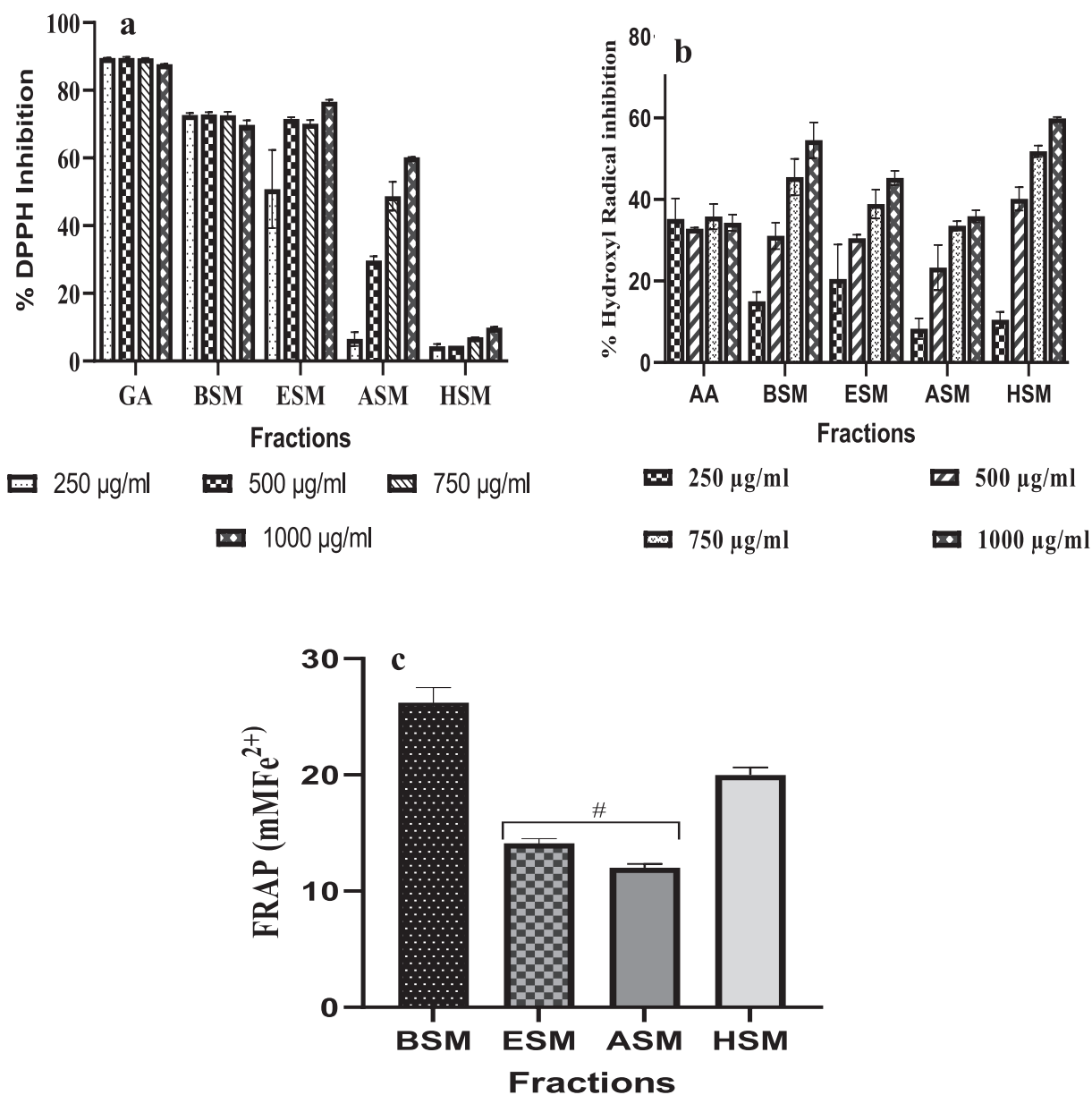


**Figure 1:** (a) Percentage DPPH inhibition (b) Percentage OH radical inhibition and (c) Ferric-reducing antioxidant power of fractions of *S. mombin* stem bark extract. AA: Ascorbic acid; GA: Gallic acid; ASM: Aqueous fraction of *S. mombin*; BSM: n-butanol fraction of *S. mombin*; ESM: Ethyl acetate fraction of *S. mombin*; HSM: n-hexane fraction of *S. mombin*. #[P < 0.05]; significant compared with BSM.

selection for further *in vivo* study. The results of this study are in accordance with the report of Ojo et al.,<sup>30</sup> who reported higher percentage inhibition of  $\alpha$ -amylase in BMS and ESM.

#### HPLC analyses of BSM

The results of the HPLC study of BSM showed the presence of eight flavonoids in the increasing concentration order of quercetin > rutin > rhamnetin > chlorogenic

acid > zeinoxanthin > lutein > isoquercetin > rutinoid (Figure 3, Table 1). Chlorogenic acid is an insulin sensitizer that potentiates the action of insulin in a comparable manner to the therapeutic mechanism of metformin by directly inhibiting glucose-6-phosphatase activity.<sup>31</sup> Lutein reportedly protects against diabetes retinopathy due to its ability to absorb oxidizing blue light, and its antioxidant potential and ability to be stored in the retina.<sup>32</sup> Isoquercetin has shown the potential to ameliorate hyperglycemia and regulates key glucose-metabolizing

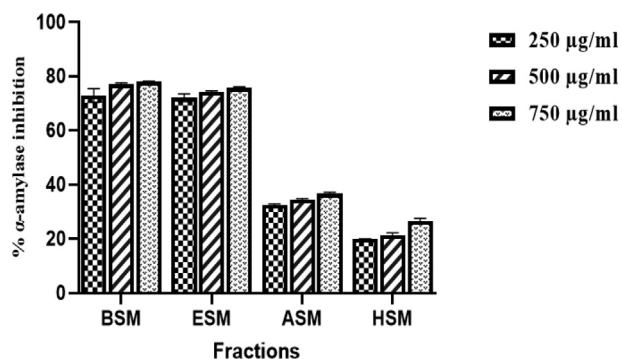


**Figure 2:** Percentage  $\alpha$ -amylase inhibition of various fractions of *S. mombin* stem bark extract. ASM: Aqueous fraction of *S. mombin*; BSM: n-butanol fraction of *S. mombin*; ESM: Ethyl acetate fraction of *S. mombin*; HSM: n-hexane fraction of *S. mombin*. # $[P < 0.05]$ ; significant compared with 250  $\mu\text{g/mL}$ .

enzymes via the insulin signaling pathway in streptozotocin-induced diabetic rats.<sup>33</sup> Rutin is a bioflavonoid present in many medicinal plants and food with neuroprotection and antidiabetic activities.<sup>34</sup> The previously reported

antidiabetic activity of the bioactive compounds identified in the BSM might be responsible for the observed antidiabetic efficacy reported in this study.

#### *Effects of ESM and BSM on the climbing and survival rates of diabetic flies*

After 45 days, the flies fed diets mixed with 2 mg BSM/10 g diet and 2 and 3 mg ESM/10 g of diet showed a non-significant ( $P > 0.05$ ) increase in the percentage survival of flies compared with flies fed 1 mL ethanol/10 g diet (Figure 4). This result justified the concentration of fractions used in this study. A significant ( $P < 0.05$ ) increase was observed in the climbing (locomotor) activity of normal flies and diabetic flies treated with ESM- and BSM-incorporated diets compared with diabetic flies without treatment (Figure 5). The significant ( $P < 0.05$ ) reduction in locomotor activity of diabetic flies without treatment was confirmed by a report that insulin resistant diabetes causes peripheral neuropathy, which includes weakness of the muscles, loss of coordination, and loss of reflexes especially of the legs.<sup>35</sup> The rescue activity of ESM and BSM fractions might be due to their antioxidant activity.

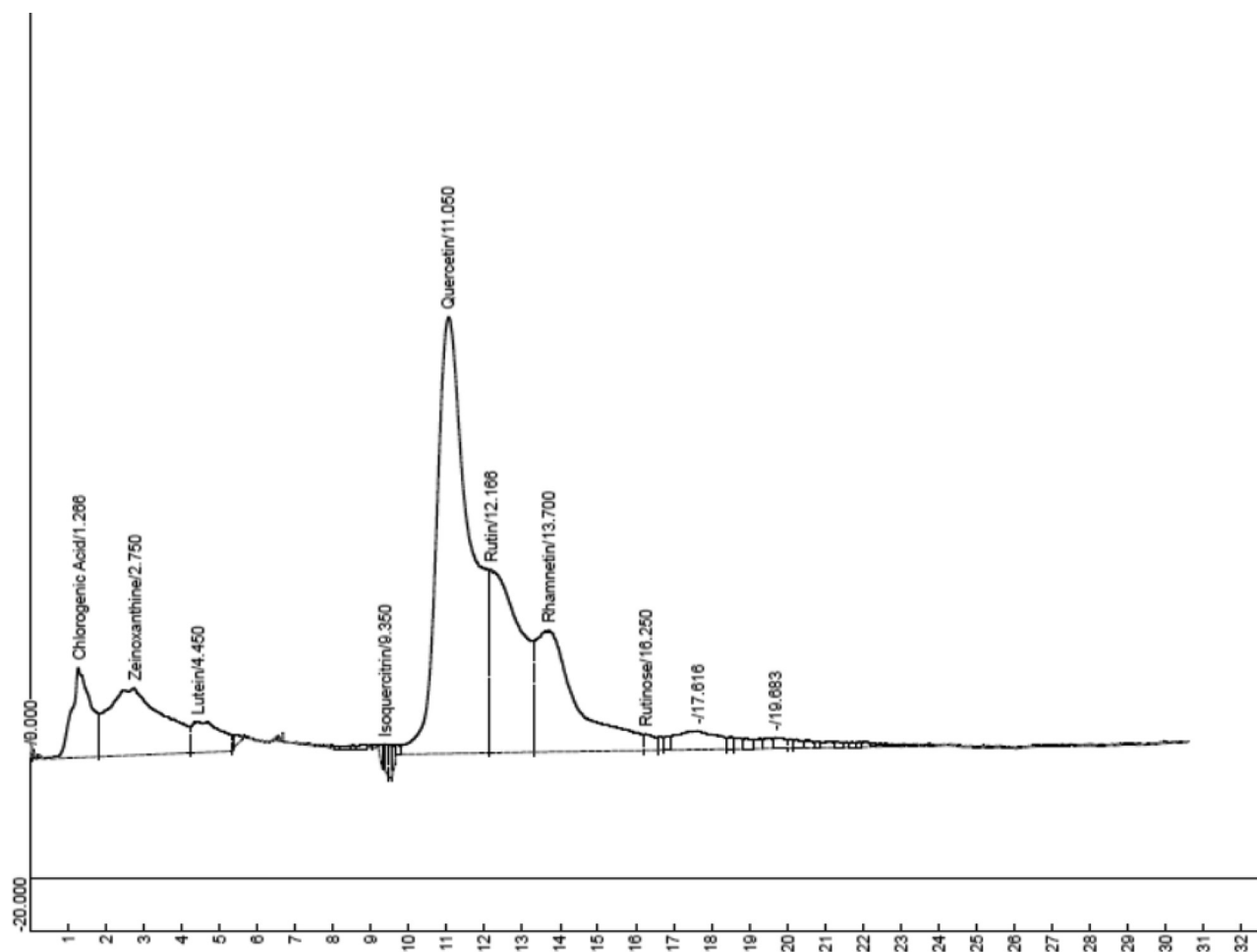


**Figure 3:** Chromatogram of HPLC compounds identified from BSM.

**Table 1: Flavonoids identified in the BSM.**

Retention time	Compounds	Height
1.266	Chlorogenic acid	33.461
2.750	Zeinoxanthin	24.967
4.450	Lutein	11.447
9.350	Isoquercetin	9.050
11.050	Quercetin	162.603
12.166	Rutin	68.379
13.700	Rhamnetin	45.298
16.250	Rutinose	6.176

#### In vivo antioxidant activity and glucose concentration of diabetic and normal flies treated with ESM and BSM

The glucose concentration of the normal and diabetic flies treated with ESM and BSM was carried out using the glucosidase method. The results showed that normal flies with or without BSM- and ESM-incorporated diets showed a significant ( $P < 0.05$ ) reduction in glucose concentration compared with flies induced with HSD only (Figure 6d). Treatment of diabetic flies with ESM and BSM significantly ( $P < 0.05$ ) reduced the glucose concentration compared with HSD-induced flies but above the glucose concentration of normal flies. The antidiabetic effect observed in the fractions was comparable to that of the standard drug metformin. Therefore, the fractions may possess a similar mode of action as metformin. The results observed in this study are in accordance with the report of Omale et al.,<sup>13</sup> who reported the glucose-lowering effect of *Parinari curatellifolia* stem bark in HSD-induced flies.

The pathogenic complications in diabetes have been associated with the generation of free radicals. Hence, the effects of ESM and BSM on selected oxidative stress markers (e.g., total thiols, NO, and lipid peroxidation) in HSD-

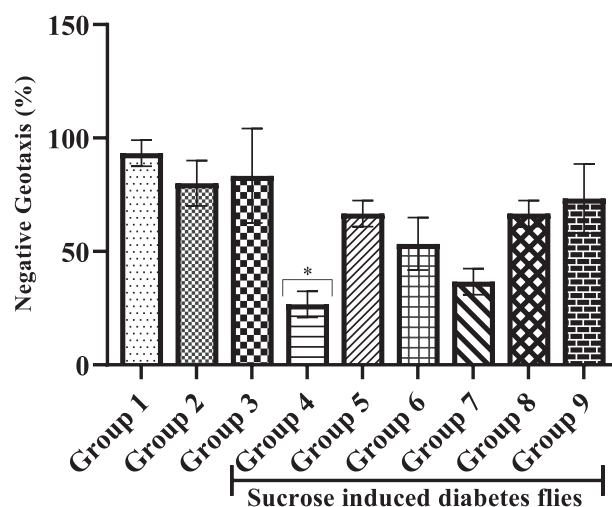


**Figure 5:** Locomotor (climbing) activity of diabetes and normal *D. melanogaster* treated with ESM and BSM. \*[ $P < 0.05$ ] significant compared to the normal control (Group 1).

induced diabetes flies was investigated. NO is a vital regulatory molecule with cellular and metabolic effects; therefore, regulating NO metabolism is vital in type 2 diabetes since activation of NO synthase is influenced by insulin.<sup>36</sup> Elevation of NO concentration with high lipid peroxidation as observed in Figure 6a and b signifies oxidative damage. The ability of ESM and BSM to appreciably reduce NO and MDA levels in HSD-induced diabetic flies further confirmed their antioxidant potential. The decrease in total thiol concentration of diabetic flies is in agreement with the results of Prakash et al.,<sup>37</sup> who showed that ESM and BSM restored the total thiol level in diabetic flies. Omale et al.<sup>38</sup> reported similar findings in *Pleurotus ostreotusto* extract.

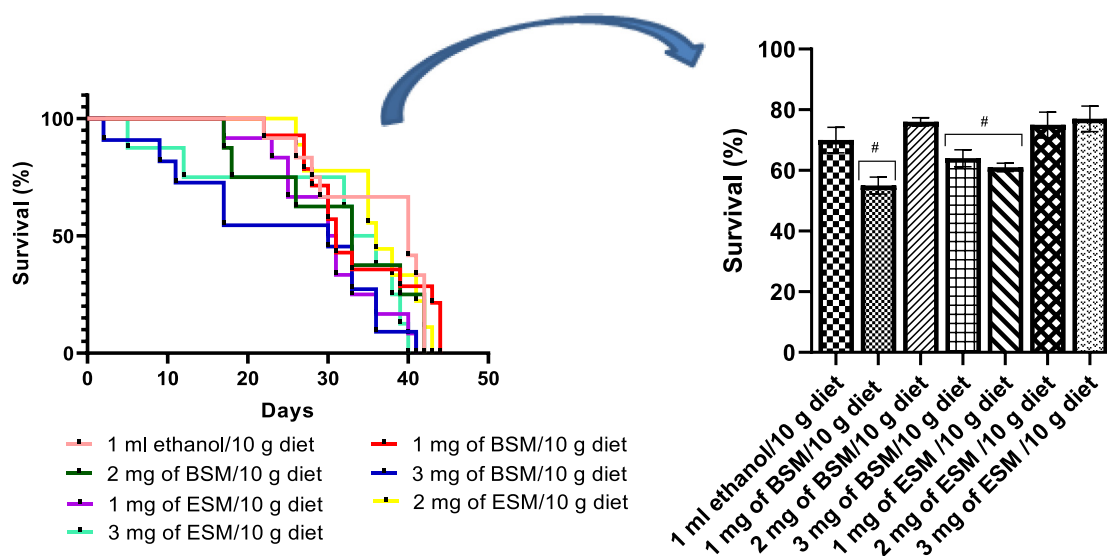


**Figure 4:** Percentage survival of *D. melanogaster* treated with *S. mombin* stem bark fractions. #[ $P < 0.05$ ]; significant compared with 1 mL ethanol/10 g diet.



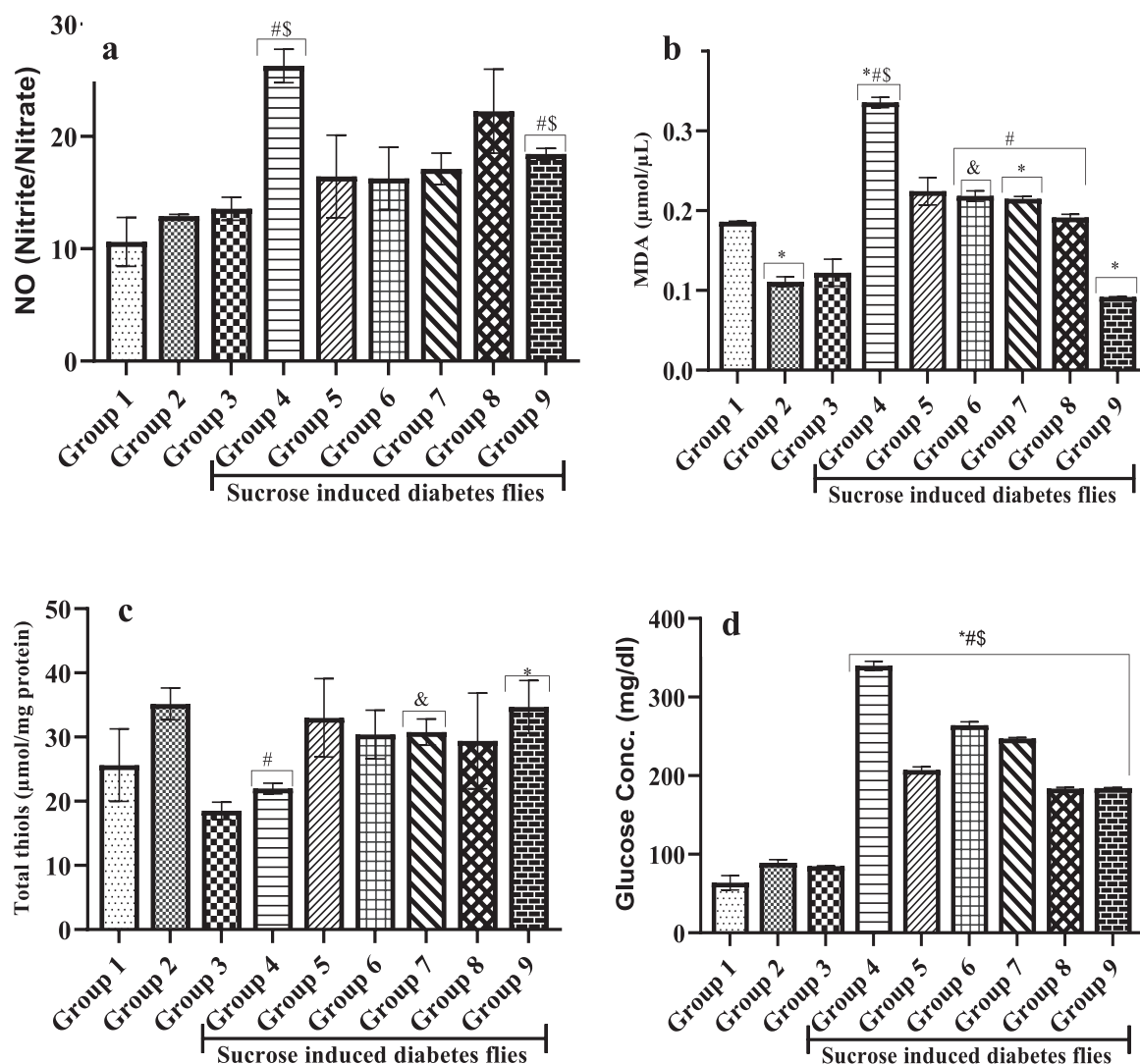


**Figure 6:** (a) NO level (b) Lipid peroxidation level (c) Total thiol level and (d) glucose concentration of diabetic and normal *D. melanogaster* treated with ESM and BSM. \* $[P < 0.05]$  significant compared to the normal control (Group 1); <sup>#</sup> $[P < 0.05]$  significant compared with Group 2; <sup>&</sup> $[P < 0.05]$  significant compared with Group 3.

#### Expression of *D. melanogaster* glucose-metabolizing genes

The potential use of *D. melanogaster* for the type 2 diabetes study was confirmed by the results obtained for the mRNA expression of glucose metabolism genes in the flies. Vertebrates such as *D. melanogaster* have one insulin gene, and *Drosophila* secretes several insulin-like peptides from insulin-producing cells (IPCs) within the brain.<sup>39</sup> The mRNA expression of three (ILP-2, InR, and IMPL2) of these peptides was evaluated to confirm the antidiabetic efficacy of ESM and BSM in HSD-induced *Drosophila*. Interestingly, the flies fed an HSD diet without fractions or drug had the downregulation of ILP-2, InR, and IMPL2 mRNA expression compared with normal and diabetic flies

fed ESM- and BSM-incorporated diets (Figure 7a–c). ILP-2 is expressed in the imaginal disc and salivary gland.<sup>40</sup> It has the highest homology with the vertebrate insulin genes, synthesized together with ILP-1, ILP-3, and ILP-5 in the IPCs within the brain and activates the insulin pathway in the fat body.<sup>39</sup> Therefore, ILP-2 regulates the metabolism of sugar and protein in response to dietary intake.<sup>41</sup> Therefore, upregulation of the gene observed in normal and HSD-induced flies fed ESM- and BSM-incorporated diets (Figure 7a) suggested an increase in the metabolism of biomolecules in the flies. Normal and HSD-induced diabetic flies fed ESM- and BSM-incorporated diets also showed the significant ( $P < 0.05$ ) upregulation of InR genes compared with diabetic flies (Figure 7b). Failure of the InR

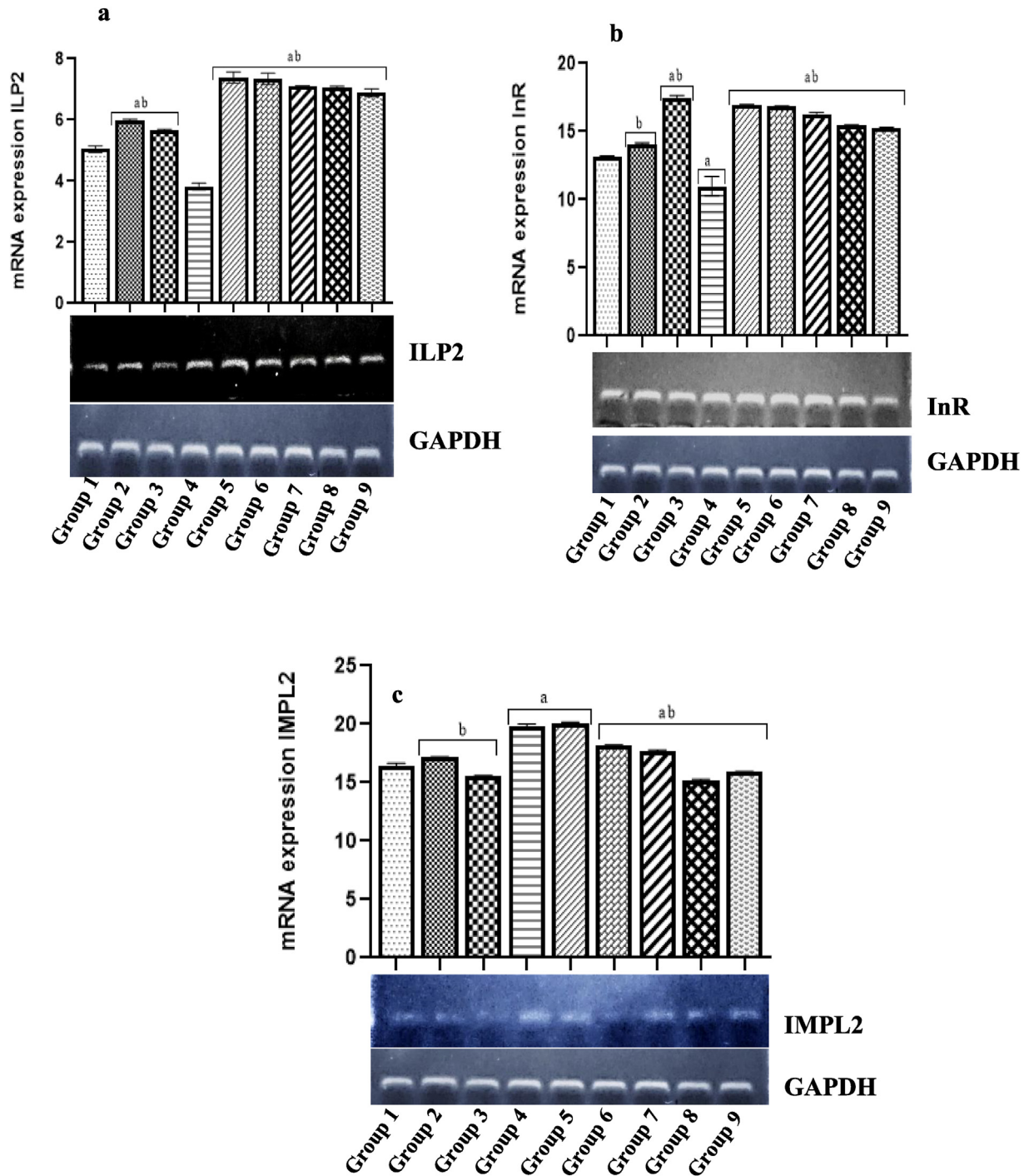


**Figure 7:** (a) ILP-2, (b) InR and (c) IMPL-2 mRNA expression of diabetes and normal *D. melanogaster* treated with ESM and BSM <sup>a</sup>[P < 0.05] significant compared with Group 1; <sup>b</sup>[P < 0.05] significant compared with Group 4.

causes insulin resistance as a result of damage to the  $\beta$ -cell. Therefore, upregulation of the InR in diabetic-treated flies might promote glucose tolerance. In *Drosophila*, the homology is IMPL2 is an insulin-growth factor that serves a regulatory function by inhibiting hunger in diabetes.<sup>42</sup> The upregulation of this gene in HSD-induced flies fed ESM-

and BSM-incorporated diets showed the ability of these fractions to activate InR and increase the release of ILP-2. The findings in this study are consistent with the upregulation of ILP-2, InR, and IMPL2 genes reported in *D. melanogaster* fed an HSD supplemented with *Artocarpus camansi* extract.<sup>43</sup>

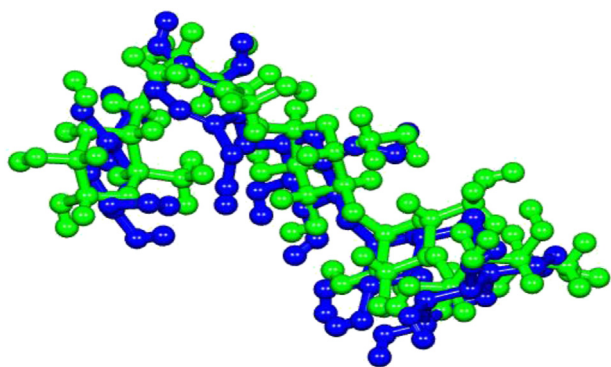


**Figure 8:** The binding conformation of co-crystallized (green) and redocked (blue) ligands at the catalytic site of  $\alpha$ -amylase (2QV4)

**Table 2: Analysis of the docked complexes.**

Entry Name	Docking score (kcal/mol)	No H-bonds	Other interactions
Chlorogenic acid	-7.8	6	4
Zeinoxanthin	-6.4	—	2
Lutein	-6.3	1	5
Isoquercetin	-8.4	6	3
Quercetin	-7.8	4	6
Rutin	-7.9	2	1
Rhamnetin	-8.0	—	7
Rutinose	-6.7	6	2
Acarbose (standard)	-7.2	6	6

#### Molecular docking of identified compounds from *S. mombin* against $\alpha$ -amylase

Molecular docking is an important tool in drug design and discovery. It suggests the effective interaction mechanism of small molecules for the binding site of the targeted receptor.<sup>44</sup> The docking procedure was validated by superimposition of extracted co-crystallized ligands from the crystallographic structure of the protein. The root mean square deviation of the redocked ligands (blue) from the co-crystallized ligand (green) in the same binding pocket of  $\alpha$ -amylase was 0.868 Å (>2.0 Å) (Figure 8).

To predict potent antidiabetic molecules with high binding affinity against the binding pocket of  $\alpha$ -amylase, the compounds identified from the HPLC chromatogram of BSM were docked against  $\alpha$ -amylase using AutoDoc vina. Table 2 shows the results of docking analysis of *in silico* antidiabetic potential of the identified compounds from *S. mombin* stem bark. The compounds showed varying degrees of binding affinities for  $\alpha$ -amylase: rhamnetin, quercetin, rutin, isoquercetin, and chlorogenic acid had higher docking scores against  $\alpha$ -amylase than the standard ligand (acarbose). The ligands interacted with various amino acids present in the binding pockets of  $\alpha$ -amylase with different molecular interactions such as van der Waals, hydrogen bond, and pi–pi stacked (Figure 9). The interaction of small

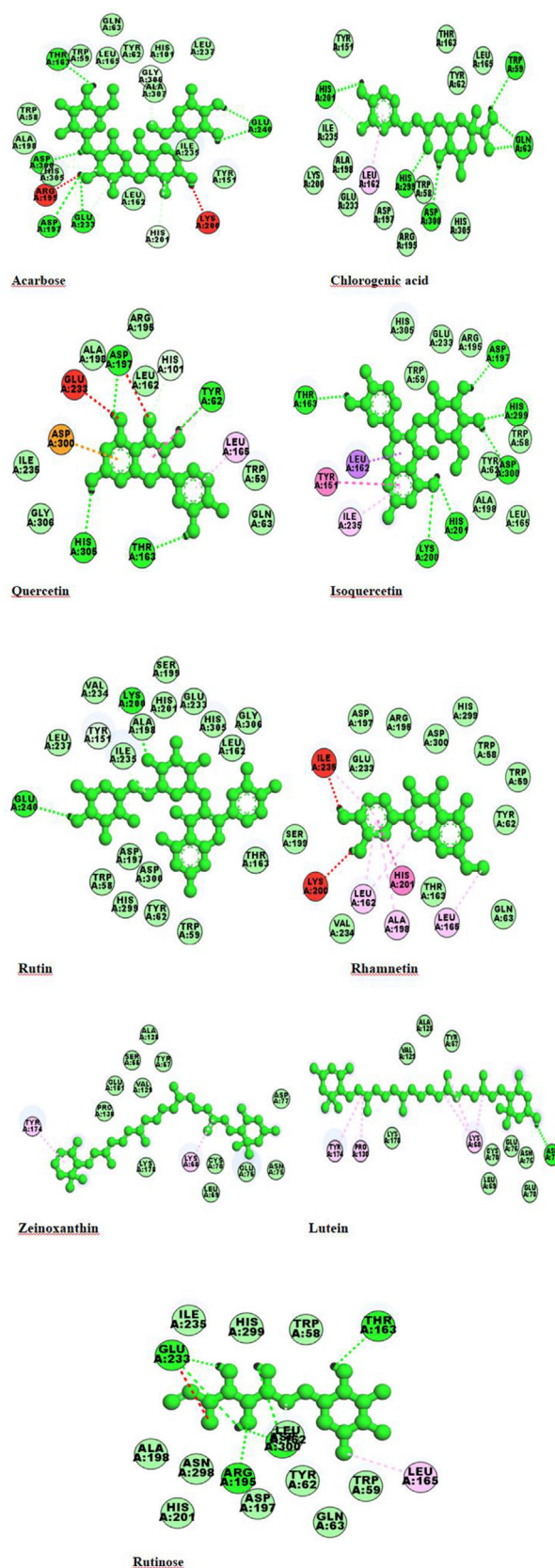


**Figure 9:** Two-dimensional presentation of interactions of compounds with catalytic pocket of  $\alpha$ -amylase (2QV4).

molecules with the amino acid at the binding site of target is vital for the inhibition of such protein.<sup>45</sup>

## Conclusion

From our observations, n-butanol and ethylacetate fractions of *S. mombin* stem bark exhibit antioxidant property to scavenge reactive oxygen species, improved survival rate, rescued locomotor performance and restored glucose homeostasis in high sucrose diet induced *D. melanogaster*. Up-regulation of ILP2, InR and IMPL2 mRNA expression was observed in diabetes and non-diabetes flies fed with diet incorporated with n-butanol and ethylacetate fractions of *S. mombin* stem bark compared with diabetes flies fed with normal diet. The inhibition of  $\alpha$ -amylase was proposed as the mechanism of anti-diabetes action from the *in vitro* and *in silico* inhibitory prediction of the active compounds identified from the HPLC chromatogram of *S. mombin* stem bark. Overall, the n-butanol and ethylacetate fractions of *S. mombin* stem bark demonstrated antioxidant and anti-diabetes efficacy in high sucrose diet induced *D. melanogaster*. It would be interesting to isolate these active compounds from *S. mombin* stem bark and test their potency in rescuing diabetes in other animal models before clinical trial of this plant part.

## Source of funding

This research did not receive any specific grant from funding agencies in the public, commercial, or not-for-profit sectors.

## Conflict of interest

The authors have no conflict of interest to declare.

## Ethical approval

Not applicable.

## Authors' contributions

DAO designed the study. DAO, SAS, and MDA conducted the methodology. DAO, SAS, and JAS provided the materials. DAO analyzed and interpreted the results. DAO and OAS drafted the manuscript. All authors have critically reviewed and approved the final draft and are responsible for the content and similarity index of the manuscript.

## References

1. Skyler JS. Diabetes mellitus: pathogenesis and treatment strategies. *J Med Chem* 2004; 47: 4113–411747.
2. Omoboyowa DA, Karigidi KO, Aribigbola TC. Nephro-protective efficacy of *Blighia sapida* stem bark ether fractions on experimentally induced diabetes nephropathy. *Comp Clin Pathol* 2021. <https://doi.org/10.1007/s00580-020-03186-w>.
3. Matsuda H, Murakami T, Yashiro K, Yamahara J, Yoshikawa M. Antidiabetic principles of natural medicines. IV. Aldose reductase and alpha-glucosidase inhibitors from the roots of *Salacia oblonga* Wall. (Celastraceae): structure of a new friedelane-type triterpene, kotalagenin 16-acetate. *Chem Pharm Bull* 1999; 17: 25–29.
4. Omoboyowa DA, Afolabi FO, Aribigbola TC. Pharmacological potential of methanol extract of *A. occidentale* stem bark on alloxan-induced diabetes rats. *Biomedical Res Ther* 2018; 5(7): 2440–2454.
5. Bai Y, Li K, Shao J, Juo Q, Jin LH. *Flos Chrysanthemi indicis* extract improves a high-sucrose diet-induced metabolic disorder in *Drosophila*. *Exp Ther Med* 2018; 16: 2564–2572.
6. Khan TA, Sievenpiper JL. Controversies about sugars: results from systematic reviews and meta-analyses on obesity, cardiometabolic disease and diabetes. *Eur J Nutr* 2016; 55: S25–S43.
7. Graham P, Pick L. *Drosophila* as a model for diabetes and diseases of insulin resistance. *Curr Top Dev Biol* 2017; 121: 397–419.
8. Osuntokun OT. Exploring the medicinal efficacy, properties and therapeutic uses of *Spondias mombin* (Linn). *J Appl Res Med Plants* 2019; 2: 115–120. <https://doi.org/10.29011/IJARMP-115.100115>.
9. Iwu MM. *Handbook of African medicinal plants*. Boca Raton: CRC Press; 1993. p. 435.
10. Fred-Jaiyesimi A, Abo K. Antidiabetic activity of *Spondias mombin* extract in NIDDM rats. *Pharmaceut Biol* 2009; 47(3): 215–218.
11. Gobinath R, Parasuraman S, Sreeramanan S, Enugutti B, Chinni SV. Antidiabetic and antihyperlipidemic effects of methanolic extract of leaves of *Spondias mombin* in Streptozotocin induced Diabetic Rats. *Front Physiol* 2022; 13:870399. <https://doi.org/10.3389/fphys.2022.870399>.
12. Gbolade AA. Effects of *Spondias mombin* stem bark and *Senna alata* leaf extracts on some biochemical parameters in rats. *J Pharm Bioresour* 2010; 7(1): 1–8. <https://doi.org/10.4314/jpb.v7i1.67746>.
13. Omale S, Aguiyi JC, Adekunle OG, Johnson TO, Ochala SO, Etuh MA, et al. Evaluation of the anti-diabetes effects of the stem bark extract of *Parinari curatellifolia* (Planch. Ex Benth) in *Drosophila melanogaster*. *J Pharmacol Toxicol* 2021; 16(1): 9–21.
14. Benzie F, Strain JJ. The ferric reducing ability of plasma (FRAP) as a measure of “antioxidant power”: the FRAP assay. *Anal Biochem* 1996; 239: 70–76.
15. Omoboyowa DA, Karigidi KO, Aribigbola TC. *Bridelia ferruginea* Benth leaves attenuates diabetes nephropathy in STZ-induced rats via targeting NGAL/KIM-1/cystatin c gene. *Clin Phytosci* 2020; 6: 63.
16. Kunchandy E, Rao MNA. Oxygen radical scavenging activity of curcumin. *Int J Pharm* 1990; 58: 237–240.
17. Worthington V. *Alpha amylase. Worthington enzyme manual*. New Jersey, United States: Worthington Biochemical Corporation; 1993. pp. 36–41.
18. Adedara AO, Babalola AD, Stephano F, Awogbindin IO, Olopade JO, Rocha JBT, et al. An assessment of the rescue action of resveratrol in *parkin* loss of function-induced oxidative stress in *Drosophila melanogaster*. *Sci Rep* 2022; 12: 3922–3934.
19. Trinder P. Enzymatic determination of glucose in blood serum. *Ann Clin Biochem* 1969; 6: 24.
20. Green LCD, Wagner A, Glogowski J, Skipper PL, Wishnok JS, Tannenbaum SR. Analysis of nitrate, nitrite, and [15N] nitrate in biological fluids. *Anal Biochem* 1982; 126: 131–138. [https://doi.org/10.1016/0003-2697\(82\)90118-x](https://doi.org/10.1016/0003-2697(82)90118-x).
21. Ohkawa H, Ohishi N, Yagi K. Assay for lipid peroxides in animal tissues by thiobarbituric acid reaction. *Anal Biochem*

- 1979; 95: 351–358. [https://doi.org/10.1016/0003-2697\(79\)90738-3](https://doi.org/10.1016/0003-2697(79)90738-3).
22. Elekofehinti OO, Lawal AO, Ejelonu OC, Molehin OR, Famusiwa CD. Involvement of fat mass and obesity gene (FTO) in the anti-obesity action of *Annona muricata* Annonaceae: in silico and in vivo studies. **J Diabet Metab Disord** 2020. <https://doi.org/10.1007/s40200-020-00491-7>.
23. Trott O, Olson AJ, Vina AD. Improving the speed and accuracy of docking with new scoring function, efficient optimization, and multithreading. **J Comput Chem** 2010; 2: 455–461.
24. Omoboyowa DA, Omomule OM, Balogun TA, Saibu OA, Metibemu DS. Protective potential of ethylacetate extract of *Abrus precatorius* seeds against HCl/EtOH-induced gastric ulcer via pro-inflammatory regulation: in vivo and in silico studies. **Phytomed Plus** 2021; 1: 10–145.
25. Grover JK, Yadav S, Vats V. Medicinal plants of India with anti-diabetes potential. **J Ethnopharmacol** 2002; 81(1): 81–100.
26. Metibemu DS, Akinloye OA, Akamo AJ, Okoye JO, Ojo DA, Morifi E, et al. Carotenoid isolates of *Spondias mombin* demonstrate anticancer effects in DMBA-induced breast cancer in Wistar rats through X-linked inhibitor of apoptosis protein (XIAP) antagonism and anti-inflammation. **J Food Biochem** 2020:e13523. <https://doi.org/10.1111/jfbc.13523>.
27. Alam MN, Bristi NJ, Rafiquzzaman M. Review on in vivo and in vitro methods evaluation of antioxidant activity. **Saudi Pharmaceut J** 2013; 21: 143–152.
28. Omoboyowa DA, Olugbenga ST, Adetuyi FD, Akinsulure ST, Akinwande KM, Iwuji CB, et al. Modulatory effects of selected compounds on oxidative stress in hydrogen peroxide-induced *Drosophila melanogaster*. **Pharm Res Modern Chin Med** 2022; 5:100169.
29. Boni ANR, Ahua KM, Kouassi K, Yapi H, Djaman AJ, Nguessan JD. Comparison of in-vitro antioxidant activities and total phenolic contents in water and methanol extracts of stems bark of *Spondias mombin*. **Res J Pharm Biol Chem Sci** 2014; 5(3): 1457–1470.
30. Ojo OA, Ajiboye BO, Imiere OD, Adeyolu O, Olayide I, Fadaka A. Antioxidative properties of *Blighia sapida* K.D. Koenig stem bark extract and inhibitory effects on carbohydrate hydrolyzing enzymes associated with non-insulin dependent diabetes mellitus. **Pharmacog J** 2018; 10(2): 376–383.
31. Meng S, Cao J, Feng Q, Peng J, Hu Y. Roles of chlorogenic acid on regulating glucose and lipids metabolism: a review. **Evid Based Complement Alternat Med** 2013; 13:801457. <https://doi.org/10.1155/2013/801457>.
32. Sahli M, Klein R, Mares JA, Meyers KJ, Ochsbalcom HM, Brady WE, et al. Associations between dietary intake of lutein and diabetic retinopathy in atherosclerosis risk in communities (ARIC) study. **Invertigat Ophthalmol Visual Sci** 2014; 55(13): 3491–3501.
33. Jayachandran M, Zhang T, Ganesan K, Xu B, Chung SSM. Isoquercetin ameliorates hyperglycemia and regulates key enzymes of glucose metabolism via insulin signaling pathway in STZ induced diabetic rats. **Eur J Pharmacol** 2018; 829: 112–120.
34. Hasanein P, Emamjomeh A, Chenarani N, Bohlooli M. Beneficial effects of rutin in diabetes-induced deficits in acquisition learning, retention memory and pain perception in rats. **Nutr Neurosci** 2020; 23(7): 563–574.
35. Bansal V, Kalita J, Misra UK. Diabetes neuropathy. **Postgrad Med** 2006; 82: 95–100.
36. Tessari P, Cecchat D, Cosma A, Vettore M, Coracina A, Million R, et al. Nitric acid synthesis is reduced in subjects with type-2 diabetes and nephropathy. **Diabetes** 2010; 59(9): 2152–2159.
37. Prakash M, Shetty MS, Tilak P, Anwar N. Total Thiols: biomedical importance and their alteration in various disorders. **Online J Health Allied Sci** 2009; 8(2): 2–12.
38. Omale S, Aguiyi JC, Bukar BB, Ede SO, Amagon KI, Amagon L, et al. Fruiting body of *Pleurotus Ostreatus* reduces serum glucose and modifies oxidative stress in type 2 diabetic: *Drosophila melanogaster* (Fruit-Fly). **Adv Pharmacol Pharm** 2020; 8(3): 41–50. 2020.
39. Álvarez-Rendón JP, Salceda R, Riesgo-Escovar JR. *Drosophila melanogaster* as a model for diabetes type 2 progression. **Bio-Med Res Int** 2018; 14:17528. <https://doi.org/10.1155/2018/1417528>.
40. Teleman AA. Molecular mechanisms of metabolic regulation by insulin in *Drosophila*. **Biochem J** 2010; 425(1): 13–26. 2010.
41. Post S, Tatar M. Nutritional geometric profiles of insulin/IGF expression in *Drosophila melanogaster*. **PLoS One** 2016; 11(5): e0155628.
42. Honegger B, Galic M, Kohler K. Imp-L2, a putative homolog of vertebrate IGF-binding protein 7, counteracts insulin signaling in *Drosophila* and is essential for starvation resistance. **J Biol** 2008; 7(3): 23–36.
43. Saliu JA, Olajuyin AM, Akinnubi A. Modulatory effect of *Artocarpus camansi* on *ILP-2*, *InR*, and *Imp-L2* genes of sucrose-induced diabetes mellitus in *Drosophila melanogaster*. **Comp Biochem Physiol, C** 2021; 246:109041.
44. Omoboyowa DA. Exploring molecular docking with E-pharmacophore and QSAR models to predict potent inhibitors of 14 $\alpha$ -demethylase protease from *Moringa* spp. **Pharm Res Modern Chin Med** 2022; 4:100147.
45. Rampogu S, Baek A, Zeb A, Lee KW. Exploration for novel inhibitors showing back-to-front approach against VEGFR-2 kinase domain (4AG8) employing molecular docking mechanism and molecular dynamics simulations. **BMC Cancer** 2018; 18: 264.

**How to cite this article:** Omoboyowa DA, Agoi MD, Shodehinde SA, Saibu OA, Saliu JA. Antidiabetes study of *Spondias mombin* (Linn) stem bark fractions in high-sucrose diet-induced diabetes in *Drosophila melanogaster*. *J Taibah Univ Med Sc* 2023;18(4):663–675.